Time-domain squeezing and quantum distributions in the pulsed regime

N. H. Adamyan,[1,*] H. H. Adamyan,[2,†] and G. Yu. Kryuchkyan[1,2]
[1]*Yerevan State University, 1 A Manoogian, 375049 Yerevan, Armenia*
[2]*Institute for Physical Research, National Academy of Sciences, Ashtarak-2, 378410, Armenia*
(Received 4 November 2007; revised manuscript received 9 January 2008; published 20 February 2008)

We investigate time-dependent properties of Einstein-Podolsky-Rosen (EPR) light beams generated in a nondegenerate optical parametric oscillator (NOPO) driven by a sequence of laser pulses with Gaussian time-dependent envelopes. This investigation continues our previous analysis [H. H. Adamyan and G. Yu. Kryuchkyan, Phys. Rev. A **74**, 023810 (2006)] and involves problems of two-mode quadrature squeezing as well as intensity-difference squeezing in the time domain. The peculiarities of EPR beams are also discussed in the framework of phase-space quantum distributions. Two kinds of non-Gaussian Wigner functions, for the reduced one-mode state of periodically pulsed NOPO and for EPR beams which are combined on a one-half beam splitter are calculated numerically. We also investigate the Wigner functions of intensity-correlated twin beams following the conditional photon state-preparation scheme. It is demonstrated that the Wigner functions involve negative values in parts of the phase space for the schemes with one, two, and three photons.

DOI: 10.1103/PhysRevA.77.023820 PACS number(s): 42.50.Dv, 03.67.Mn

I. INTRODUCTION

The recent development of continuous-variable (CV) quantum information is stipulated mainly by preparation of two-mode squeezed vacuum states which are a realization of Einstein-Podolsky-Rosen (EPR) entanglement. It is recognized that a nondegenerate optical parametric oscillator (NOPO) is a suitable system for generation of these states, and hence, for demonstration of CV entanglement [1]. Indeed, CV entanglement as a two-mode squeezing was experimentally demonstrated for the first time in a NOPO operating below threshold [2]. Since this significant milestone, there have been further experimental observations of the EPR entanglement [3–5].

A type-II optical parametric oscillator pumped above threshold has also been theoretically predicted to be a very efficient source of bright entangled light [1]. The strong quantum consideration of NOPO in this operational regime showing the production of EPR states has recently been given in [6]. Entanglement in the above-threshold NOPO was last observed by three groups [7–9]. In the perspective to generate intense EPR light beams the ultrastable phase-locked type-II NOPO above threshold has been recently proposed and experimentally realized in the area of quantum optics [10–16]. Particularly, EPR entangled states under the mode phase-locked condition have been investigated in [13,14] and observed in phase-locked NOPO in [9].

In the standard treatment of the optical parametric oscillator, the pump is considered as a time-independent monochromatic beam and the calculations are performed in the frequency domain. In the CV regime, a wide variety of quantum communication applications based on EPR entangled states has been also demonstrated in the frequency domain. The usual way to measure CV entanglement is the homodyne detection in the frequency domain [2–5] which deals with only frequency sidebands a few MHz apart from the carrier frequency. Nevertheless, recent experimental achievements in quantum optics initiate investigations of EPR entanglement also in the time domain [17–22]. Such investigations may open a way for new applications in many areas of time-resolved quantum information and communications in addition to the well-known protocols already elaborated in the spectral domain. For this goal a method of time-resolved homodyne measurement has been developed following the pioneering experiment on quantum tomography [23]. This approach can be applied for measurements of the squeezing in the time domain. In this area, generation and characterization of quadrature-squeezed pulses as well as entangled light pulses in the time domain have been recently performed [17–19]. The time-domain analysis is convenient in the case when the continuous time evolution of the light generated in a NOPO is observed. A multimode treatment of OPO which is valid for both pulsed and continuous-wave pump fields has been presented in [24]. It should be also noted that the conditional one-photon and two-photon Fock states have been experimentally obtained from a pulsed nondegenerate parametric optical amplifier. These states have also been analyzed by the pulsed homodyne detection [25–27]. Another field of time-domain analysis application is the generation of non-Gaussian states in optical systems using a technique called "photon subtraction" [28]. In this approach a small fraction of the light is extracted on a beam splitter and detected using photon counting in the time domain. Note that generation of a superposition of odd photon number states from a squeezed state produced by OPO is experimentally demonstrated based on this approach [29]. In order to realize CV teleportation of such non-Gaussian states, one needs to generate EPR entanglement in the time domain. In this area, the experimental generation and characterization of a two-mode squeezed vacuum state in a time-gated way has been recently demonstrated in [22].

Thus for applications with nonclassical states, particularly, with EPR states in the time domain, a rigorous study of NOPO is needed for operating in various time-dependent regimes. As a step in this direction a periodically pulsed

*narek.adamyan@synopsys.com
†adamyan.hayk@gmail.com

NOPO, i.e., a NOPO under time-modulated pumping field, has been proposed and studied theoretically [14,21] in application to generation of EPR entangled light beams in the time domain.

In this paper we continue the investigation of periodically pulsed NOPO following Ref. [21]. Our goal is twofold. In one part of the present paper we extend our previous results [21] regarding NOPO above threshold under action of a sequence of the Gaussian pulses. The other part of the paper is devoted to calculation of dynamics of the Wigner functions for the pulsed regime of NOPO, since Wigner functions give a complete description of the states of quantum systems.

The paper is arranged as follows. In Sec. II we briefly describe the theory of periodically pulsed NOPO. Section III is devoted to analysis of EPR entanglement and intensity-difference squeezing in the time domain for NOPO under Gaussian pulses. In Sec. IV we consider EPR beams from a different perspective on the base of the Wigner functions. We calculate two types of Wigner functions, first for squeezing components of EPR beams, which are combined on a one-half beam splitter, and second for each of the subharmonic modes. In Sec. V we present theoretical analysis of non-Gaussian quantum states with negative values of $W(x,p)$ generated on periodically pulsed NOPO. The various state-preparation schemes counting $n=1$, $n=2$, and $n=3$ photons are considered. We summarize our results in Sec. VI.

II. PERIODICALLY PULSED NOPO: BRIEF DESCRIPTION

In this section we briefly describe a type-II phase-matched NOPO with a triply resonant optical ring cavity driven by a periodic sequence of laser pulses. The semiclassical and quantum theories of time-modulated NOPO were developed in Refs. [14,21] and here we only add some important details regarding the case of laser pulses with Gaussian time-dependent envelopes.

Thus, we consider the NOPO based on intracavity parametric interaction between pump mode [labeled as (3)] and two subharmonic modes [(1) and (2)] of orthogonal polarizations. These modes have plane polarizations and are all propagating in the same direction. The pump mode at the central frequency $\omega_3=\omega_L$ is driven by a periodically pulsed laser field.

We assume in-field as nonstationary Gaussian pulses which can be written in the following form:

$$E_L(t,z)=\int_{-\infty}^{\infty}\varepsilon_L(t,z,\omega)d\omega, \tag{1}$$

where in one-nonmonochromatic mode approximation and for the case of a single pulse

$$\varepsilon_L(t,z,\omega)=\frac{1}{\sqrt{2\pi\sigma^2}}E_{0L}e^{-\omega^2/2\sigma^2}e^{-i(\omega+\omega_L)t}e^{ik_Lz}, \tag{2}$$

i.e., it is defined as a classical pump beam with Gaussian frequency envelope of full-width at half-maximum bandwidth $\Delta\omega=\sigma$ and central frequency ω_L. The Gaussian function $e^{-\omega^2/2\sigma^2}$ is the weight of the component $\omega+\omega_L$ of the pulse. Thus, the time-dependent field is

$$E_L(t,z)=E_{0L}e^{-t^2/T^2}e^{-i(\omega_Lt-k_Lz)}, \tag{3}$$

where $T=\sqrt{2}/\sigma$.

We consider below the case of the Gaussian pulses separated by the time intervals τ. The corresponding time-dependent field is

$$E_L(t,z)=E_{0L}f(t)e^{-i(\omega_Lt-k_Lz)}, \tag{4}$$

$$f(t)=\sum_{n=-\infty}^{\infty}e^{-(t-t_0-n\tau)^2/T^2}. \tag{5}$$

In this regime the dynamics of the intracavity modes, which are the pump mode and the modes of subharmonics, are also pulsed. Therefore, at the quantum level, we use a specific second-quantization form of the intracavity field operators in the terms of pulse modes, i.e., we consider the expansion of the field operators through the time-dependent amplitudes defining the wave-packet envelopes of the intracavity modes and the annihilation mode operators b_n. The pump mode described by the operator b_3 is driven by the amplitude-modulated external field at the central frequency $\omega_L=\omega_3$. The parametric interaction leads to a generation of pair correlated pulses of orthogonal polarization in the $\chi^{(2)}$ medium, which are described by the operators b_1 and b_2.

We assume wideband collinear phase matching which can be more effectively realized in a periodically poled crystal. The basic energy conservation for the central frequencies and perfect phase matching imply that $\omega_L\rightarrow\omega_1(\uparrow)+\omega_2(\rightarrow)$, $\omega_1=\omega_2=\frac{\omega_L}{2}$, and $\Delta k=k_L(\omega_L)-k_1(\omega_1)-k_2(\omega_2)-k_g=0$, where k_g is the poling wave vector. The corresponding interaction Hamiltonian within the framework of the rotating wave approximation and in the interaction picture is

$$H=i\hbar\chi f(t)(e^{i\Phi_L}b_3^{\dagger}-e^{-i\Phi_L}b_3)+i\hbar k(e^{i\Phi_k}b_3b_1^{\dagger}b_2^{+}-e^{-i\Phi_k}b_3^{\dagger}b_1b_2), \tag{6}$$

where χ is the coupling constant of the in field with the ω_3-intracavity mode which is proportional to the amplitude E_{0L} of the pump field and constant $ke^{i\Phi_k}$ determines the efficiency of the parametric process.

Note that the operators b_n $(n=1,2,3)$ are intracavity envelope operators for pump (b_3) and subharmonic modes (b_1), (b_2) which satisfy the commutation relations, $[b_n,b_m^{\dagger}]=\delta_{nm}$. Such discrete mode operators [30,31] are more suitable for complete quantum description of pulsed dynamics than usual continuous bosonic operators that satisfy the commutation relation $[a(t),a^{\dagger}(t')]=\delta(t-t')$. This approach has recently been used also for complete quantum description of both the process of a down conversion and NOPO in pulsed regimes [24,31–34]. A thorough discussion of continuous and discrete operator description of light beams in both time and frequency space may be found in [35].

The master equation for the reduced density matrix of the nonmonochromatic modes and for the case of zero detuning is obtained as

$$\frac{\partial \rho}{\partial t} = \frac{1}{i\hbar}[H,\rho] + \sum_{i=1}^{3} \gamma_i (2b_i \rho b_i^* - b_i^\dagger b_i \rho - \rho b_i^\dagger b_i), \qquad (7)$$

where γ_1, γ_2, and γ_3 are the damping rates of modes ω_1, ω_2, and ω_3. We consider below the case of high cavity losses for the pump mode ($\gamma_3 \gg \gamma, \gamma_1 = \gamma_2 = \gamma$), when the pump mode is eliminated adiabatically. In this regime, the stochastic equations of motion for the complex c-number variables α_i and β_i corresponding to the operators b_i and $b_i^\dagger$ have the following form [21]:

$$\frac{d\alpha_1}{dt} = -(\gamma + \lambda \alpha_2 \beta_2)\alpha_1 + \varepsilon(t)\beta_2 + W_{\alpha_1}(t), \qquad (8)$$

$$\frac{d\beta_1}{dt} = -(\gamma + \lambda \alpha_2 \beta_2)\beta_1 + \varepsilon(t)\alpha_2 + W_{\beta_1}(t). \qquad (9)$$

Here $\varepsilon(t) = f(t)\chi k/\gamma_3$, $\lambda = k^2/\gamma_3$, and the equations for α_2, β_2 are obtained from (8) and (9) by exchanging the subscript $(1) \rightleftarrows (2)$. Our derivation is based on the Ito stochastic calculus, and the nonzero correlators are

$$\langle W_{\alpha_1}(t) W_{\alpha_2}(t') \rangle = [\chi f(t) - \lambda \alpha_1 \alpha_2]/\gamma_3, \qquad (10)$$

$$\langle W_{\beta_1}(t) W_{\beta_2}(t') \rangle = [\chi f(t) - \lambda \beta_1 \beta_2]/\gamma_3. \qquad (11)$$

Note that while obtaining these equations we used the transformed boson operators $b_i \to b_i \exp(-i\Phi_i)$, being $\Phi_3 = \Phi_L$, $\Phi_1 = \Phi_2 = \frac{1}{2}(\Phi_L + \Phi_k)$. This leads to cancellation of the phases at intermediate stages of calculations.

The semiclassical and quantum analysis of Eqs. (8) and (9) have been performed in Ref. [21] in applications to two schemes of NOPO: Driven by continuously modulated pump field; and under action of a periodic sequence of rectangular laser pulses. We apply below these results for a more experimentally feasible scheme of NOPO under Gaussian laser pulses. In the other part of the paper, we numerically calculate the non-Gaussian Wigner functions for NOPO for the above threshold regime in the framework of the master equation (7).

First, we briefly discuss the mean photon number of subharmonic modes $\langle n_i \rangle = \langle b_i^\dagger b_i \rangle$ $(i = 1,2)$ in the semiclassical treatment. The analysis shows [21] that similar to the standard NOPO with stationary pump field amplitude, the periodically pulsed NOPO also exhibits threshold behavior, which is easily described through the period averaged pump field amplitude $\overline{f(t)} = \frac{1}{\tau}\int_0^\tau f(t)dt$. As shown in the Appendix, for the case of Gaussian pulses (2) and (3), an above-threshold regime is realized if

$$\chi > \chi_{\text{th}} = \frac{\gamma \gamma_3}{\sqrt{\pi k}} \frac{\tau}{T}. \qquad (12)$$

We find that as for usual NOPO, the phase difference of the generated modes ($\alpha_i = \beta_i^*$, $\alpha_i = \sqrt{n_i} e^{i\phi_i}$, $n_i = |\alpha_i|^2$) is undefined due to the phase diffusion, while the sum of phases $\phi_1 + \phi_2 = \phi_L + 2\pi m$ $(m = 0,1,2,\ldots)$. The mean semiclassical photon numbers for subharmonic modes are equal from one to the other $(n_1 = n_2 = n_c)$ due to the symmetry of the system, $\gamma_1 = \gamma_2 = \gamma$, and have been calculated in the following form:

$$n_c^{-1}(t) = 2\lambda \int_{-\infty}^{0} \exp\left(2\int_0^\tau [\varepsilon(t'+t) - \gamma] dt' \right) d\tau. \qquad (13)$$

This result is obtained for over-transient $t \gg \gamma^{-1}$ and above-threshold regimes. Typical results for two different parameters of the Gaussian pulses are presented in Fig. 1.

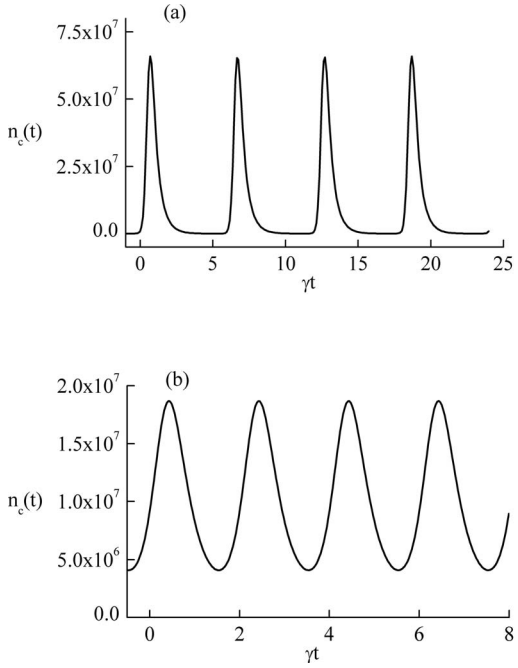

FIG. 1. Mean photon number versus dimensionless time for the following parameters: (a) $\lambda = 10^{-8}\gamma$, $\chi = 1.1\chi_{\text{th}}$, $\tau = 6\gamma^{-1}$, $T = 0.6\gamma^{-1}$; (b) $\lambda = 10^{-8}\gamma$, $\chi = 1.1\chi_{\text{th}}$, $\tau = 2\gamma^{-1}$, $T = 0.5\gamma^{-1}$.

III. EPR ENTANGLEMENT AND INTENSITY-DIFFERENCE SQUEEZING INDUCED BY GAUSSIAN PULSES

In the field of CV quantum variables it is an established standard to describe squeezing with the spectra of quantum fluctuations, as has been done even for some pulsed squeezing experiments [36]. Indeed, most of the experiments, relaying on optical intracavity interactions, have been performed for fields outside a cavity in the spectral domain. The other quantity characterizing quantum noise is the total squeezing or integrated on the spectral bandwidth squeezing which can be naturally investigated in the time domain. The usage of cavities in NOPO limits the bandwidth of squeezing or EPR correlation within the cavity bandwidth. In this section we investigate the integral two-mode squeezing for periodically pulsed NOPO. Two types of quantum noise reduction effects, the quadrature squeezing as well as the intensity-difference squeezing, are considered.

A. Time-dependent quadrature squeezing

We can construct position and momentum operators for the two modes of NOPO and the eigenvalues of these opera-

tors would define the phase space. The criterion of two-mode quadrature squeezing or EPR entanglement is formulated as $V=\frac{1}{2}[V(X_1-X_2)+V(Y_1+Y_2)]<1$ in terms of the variances of the quadrature amplitudes of two modes $X_k=X_k(\theta_k)=\frac{1}{\sqrt{2}}(b_k^\dagger e^{-i\theta_k}+b_k e^{i\theta_k})$, $Y_k=X_k(\theta_k-\frac{\pi}{2})$ $(k=1,2)$, where $V(x)=\langle x^2\rangle-\langle x\rangle^2$ is a denotation of the variance.

As it was shown theoretically, in NOPO under a continuous monochromatic pump the integral intracavity two-mode squeezing is limited, and reaches only 50% relative to the level of vacuum fluctuations, i.e., $\frac{1}{2}<V<1$ (see [37,38], for a linear treatment of quantum fluctuations and [6] for nonperturbative treatment). However, a spectral squeezing significantly lower than the integral squeezing has been achieved at definite low-frequency spectral ranges.

Nevertheless, as has been shown [21], the time modulation of pump field amplitude essentially improves the degree of squeezing in NOPO. On the whole the level of integral two-mode squeezing, which characterizes the degree of EPR entanglement, goes below the limit $V=\frac{1}{2}$ for the definite time intervals. In this section we illustrate this effect for the realistic experimental situation, that is, a NOPO under a periodic sequence of Gaussian laser pulses.

Our analysis is based on the equations that have been obtained in Ref. [21],

$$\frac{d}{dt}\langle n_+\rangle=[2\varepsilon(t)-2\gamma-\lambda]\langle n_+\rangle-\lambda\langle n_+^2\rangle-2\varepsilon(t)\langle R\rangle+\lambda\Delta, \tag{14}$$

$$\frac{d}{dt}\langle R\rangle=-[2\varepsilon(t)+2\gamma+\lambda]\langle R\rangle-\lambda\langle n_+R\rangle-2\varepsilon(t)+\lambda\Delta, \tag{15}$$

$$\frac{d}{dt}\Delta=-4\gamma\Delta+2\gamma\langle n_+\rangle \tag{16}$$

for the following time-dependent quantities: $\langle n_+\rangle=\langle b_1^\dagger b_1\rangle+\langle b_2^\dagger b_2\rangle$, $\langle R\rangle=\langle b_1^\dagger b_1\rangle+\langle b_2^\dagger b_2\rangle-\langle b_1 b_2\rangle+\langle b_1^\dagger b_2^\dagger\rangle$, and $\Delta=\langle(b_1^\dagger b_1-b_2^\dagger b_2)^2\rangle$. We apply these equations for the case of the Gaussian pump pulses, i.e., for

$$\varepsilon(t)=\frac{\chi k}{\gamma_3}\sum_{n=-\infty}^{\infty}e^{-(t-n\tau)^2/T^2} \tag{17}$$

and for the symmetrical NOPO, $\gamma_1=\gamma_2=\gamma$, where the mean photon number of subharmonic modes are equal from one to another $\langle n_1\rangle=\langle n_2\rangle=\langle n\rangle$.

In the linear treatment of quantum fluctuations the variance $V(t)=1+\langle\delta R\rangle$ obeys the following equation:

$$\frac{dV}{dt}=-2[\gamma+\varepsilon(t)+\lambda n_c]V+2\gamma+2\lambda(n_c+\Delta), \tag{18}$$

leading to the result

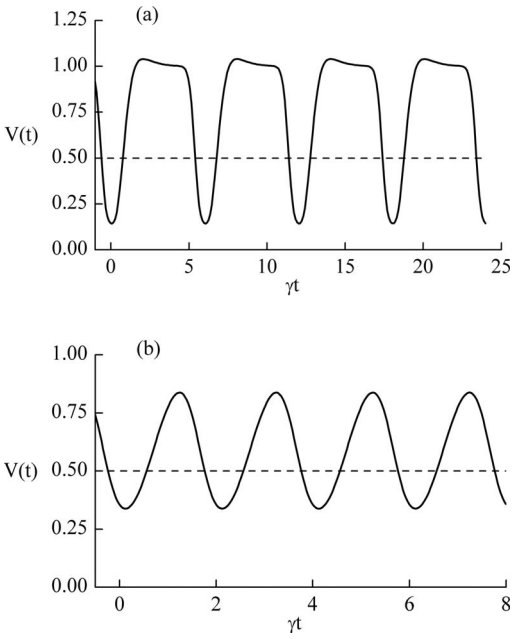

FIG. 2. Degree of two-mode squeezing versus dimensionless time for the following parameters: (a) $\lambda=10^{-8}\gamma$, $\chi=1.1\chi_{\rm th}$, $\tau=6\gamma^{-1}$, $T=0.6\gamma^{-1}$; (b) $\lambda=10^{-8}\gamma$, $\chi=1.1\chi_{\rm th}$, $\tau=2\gamma^{-1}$, $T=0.5\gamma^{-1}$.

$$V(t)=2\int_{-\infty}^{t}\exp\left(-2\int_{\tau}^{t}[\gamma+\varepsilon(t')+\lambda n_c(t')]dt'\right)\left(\gamma+\lambda_c(\tau)+2\gamma\lambda\int_{-\infty}^{\tau}e^{4\gamma(\tau'-\tau)}n_c(\tau')d\tau'\right)d\tau. \tag{19}$$

This result is obtained for an over-transient regime $t-t_0\gg\gamma^{-1}$ and in $\lambda/\gamma\ll1$ approximation for periodic on time parameter $\varepsilon(t)$ in (17). Note that in the current experiments the ratio k/γ (typically 10^{-8} or less), and hence $\lambda/\gamma=k^2/\gamma\gamma_3\ll1$ is the small parameter of the theory. This result relies on the above-threshold regime. The analysis of the below-threshold regime leads to the formula (19) with $n_c=0$.

The dependence of V versus the scaled time is shown in Fig. 2 for the parameters as in Fig. 1 and for two nonstationary regimes. The dashed lines in Fig. 2 indicate the degree of two-mode squeezing for the stationary regimes: $T\gg\gamma^{-1}$, $\tau\to0$, and $\chi=\chi_{\rm th}$. In both nonstationary regimes (a) the pulses of duration $T=0.6\gamma^{-1}$ separated by the time interval $\tau=6\gamma^{-1}$ and (b) $T=0.5\gamma^{-1}$, $\tau=2\gamma^{-1}$, the modulation of the quadrature variances repeats the periodicity of the pump laser. Figures 2(a) and 2(b) illustrate CV entanglement when duration of the pulses is close to a characteristic dissipation time. It is clearly seen that the variances for pulsed dynamics obey the EPR criterion $V^2<1/4$ for definite time intervals. We also found a remarkable result that the variance goes below the stationary limit of 0.5 in the ranges where photon number is maximal for appropriate chosen parameters. For intensity comparing Figs. 1(a) and 2(a), we conclude that for time intervals leading to the maximal photon number $n_{\rm max}=6.5\times10^7$, the corresponding variance is equal to $V=0.35$. On the other hand, the maximal variance $V_{\rm min}=0.146$ takes

place for the main photon number $n=2.5\times10^6$.

Similar conclusions hold for the output measured integral two-mode squeezing which is realized if $V^{\text{out}}=2\gamma(V-1)<0$ [30]. The lower bound for V^{out} in the stationary limit $V\geq1/2$ reads as $V^{\text{out}}/2\gamma\geq-1/2$. The above results indicate that in the periodic pulsed regimes the normalized output variance becomes less than $-1/2$, i.e., $V^{\text{out}}/2\gamma<-1/2$ for the definite time intervals.

B. Photon-number difference squeezing in the time domain

Let us now discuss photon-number correlation in the time domain, considering output twin light beams from the pulsed NOPO. The photon-number correlation of twin beams is usually characterized by the intensity-difference squeezing in the spectral domain since the presentation of Ref. [39]. In this way the intense twin beams' quantum correlations have been experimentally observed several years ago in NOPO operated above its threshold [40] and the experimental progress in this direction has been made in a series of papers [41]. It should be noted again the difference between the focus of this section and the above-mentioned papers in this area. We analyze the intensity-difference squeezing in the time domain, but not in the spectral domain.

We focus on the measurement scheme of photon-number correlation in terms of photoelectric currents of two modes $\langle i_1(t)\rangle,\langle i_2(t)\rangle$. The photocurrent difference variance $R(t)=\langle[i_1(t)-i_2(t)]^2\rangle-[\langle i_1(t)\rangle-\langle i_2(t)\rangle]^2$ in accordance with a standard theory of photoelectric detection reads as

$$R(t)=R_{\text{shot}}(t)+(2Q\alpha\gamma)^2(\langle n_1\rangle+\langle n_2\rangle)[G(t)-1], \quad (20)$$

where Q is the total charge per photopulse, α is the dimensionless quantum efficiency of detectors ($\alpha\leq1$), the shot-noise term $R_{\text{shot}}(t)$ is proportional to the sum of photon numbers $R_{\text{shot}}(t)\sim\langle n_1(t)\rangle+\langle n_2(t)\rangle=2\langle n(t)\rangle$, while $G(t)=\Delta(t)/2\langle n(t)\rangle$, $\Delta(t)=\langle(b_1^\dagger b_1-b_2^\dagger b_2)^2\rangle$.

Using Eq. (16) of periodically pulsed NOPO, the normalized variance $G(t)$ can be obtained in the following form:

$$G(t)=\frac{2\gamma}{\langle n(t)\rangle}\int_{-\infty}^{0}d\tau e^{4\gamma\tau}\langle n(t+\tau)\rangle. \quad (21)$$

Surprisingly, the variance $G(t)$ is expressed in a simple enough form and in the framework of "exact" quantum theory without restoring to a linear treatment of quantum fluctuations.

For the case of an ordinary NOPO with stationary pump amplitude, $f(t)=f_0=\text{const}$, we conclude that

$$\langle n(t)\rangle=n_s=\frac{\chi f_0-\gamma\gamma_3/k}{k}, \quad (22)$$

i.e., $\langle n(t)\rangle$ is the stationary mean photon number of the modes, and then

$$G(t)=\Delta/2\langle n\rangle=\frac{1}{2}. \quad (23)$$

Thus, in this case the variance normalized to the level of quantum fluctuations for the coherent state reaches only 50% relative to the coherent shot noise level. The late result is in agreement with the result of Ref. [42], carried out in the framework of the stationary solution of the Fokker-Planck equation.

Thus, for an ordinary NOPO under monochromatic pump, the normalized variance of the photon-number difference G is equal to $\frac{1}{2}$ for arbitrary parameters in contrast to the quadrature variance V which is a complex function of the system's parameters. Nevertheless, for the periodically pulsed NOPO the corresponding time-dependent variances $V(t)$ and $G(T)$ display the same temporal behavior for the wide range of the parameters. Indeed, using Eqs. (14) and (16) we obtain

$$\frac{dG}{dt}=\left(-2\gamma-2\varepsilon(t)+\lambda(1+\langle n_+\rangle)-2\varepsilon(t)\frac{\langle R\rangle}{\langle n_+\rangle}+\lambda G\right)G+2\gamma. \quad (24)$$

Since $\lambda G\ll\gamma$, $n_+\ll1$, and hence $\frac{\langle R\rangle}{\langle n_+\rangle}\ll1$, the equation can be simplified as

$$\frac{dG}{dt}=-2[\gamma+\varepsilon(t)-\lambda n_c]G+2\gamma. \quad (25)$$

As we show, Eqs. (18) and (25) coincide if $\lambda n_c\ll\gamma$.

This result clearly shows that looking for two-mode quadrature squeezing in the time domain for periodically pulsed NOPO above threshold is equivalent to looking for time-dependent photon-number difference squeezing.

Note that the numerical calculations on the base of the formulas (5), (13), and (21) approve of this result. In fact, as shown in our calculations, the curves for $G(t)$ are coincided with the curves (a) and (b) for $V(t)$ depicted in Fig. 2. Thus, we conclude that a demonstration of the integral CV entanglement in the time domain can be performed also by a direct measurement of the photon-number difference squeezing.

IV. WIGNER FUNCTIONS AND PROBABILITY DISTRIBUTIONS OF QUADRATURE AMPLITUDES

In this section we consider two-mode squeezed states produced in the pulsed NOPO from a different perspective on the base of quantum distributions in the phase space. We calculate numerically two kinds of Wigner functions, for the reduced, one-mode state of NOPO and for EPR beams which are combined on a one-half beam splitter. This investigation seems to be interesting in the area of pulsed homodyne detection and the so-called optical homodyne tomography. In the method of pulsed homodyne detection a single measurement of the quadrature amplitude of the signal pulse is performed for each pulse in the time domain. Therefore, the periodically pulsed NOPO is suitable for such a scheme of the measurement.

Our calculations are based on the quantum state diffusion (QSD) approach that represents the reduced density operator of two generated modes by the mean over the projectors onto the stochastic states $|\psi_\xi\rangle$ of the ensemble $\rho(t)=M(|\psi_\xi\rangle\langle\psi_\xi|)$, where M denotes the ensemble averaging. The corresponding equation of motion is

$$|d\psi_\xi\rangle = -\frac{i}{\hbar}H|\psi_\xi\rangle dt + \frac{1}{2}(L^\dagger L + \langle L^\dagger\rangle\langle L\rangle - 2\langle L^\dagger\rangle L)|\psi_\xi\rangle dt + (L - \langle L\rangle)|\psi_\xi\rangle d\xi, \quad (26)$$

where ξ indicates the dependence on the stochastic process, the complex Wiener variable $d\xi_i$ satisfies the fundamental properties $M(d\xi_i)=0$, $M(d\xi_i d\xi_j)=0$, $M(d\xi_i d\xi_j^*)=\delta_{ij}dt$, and the expectation value $\langle L_i\rangle=\langle\psi_\xi|L_i|\psi_\xi\rangle$.

First, we calculate Wigner functions based on QSD for each of the individual (signal or idler) modes. This is obtained by integrating the two-mode Wigner function $W(\alpha_1,\alpha_2)$ over one of the phase-space variables α_1 or α_2 corresponding to the operators b_1 and b_2. Due to the symmetry of the $W(\alpha_1,\alpha_2)$ with respect to α_1 or α_2, the one-mode Wigner functions for the signal and the idler modes are equal to each other and can be represented as

$$W_1(\alpha) = \int d^2\alpha_2 W(\alpha_1,\alpha_2). \quad (27)$$

We calculate $W_1(\alpha)$ by using the reduced density operators for each of the modes which are constructed from the density operator ρ of both modes by tracing over one of the modes $\rho_{1(2)}=\mathrm{Tr}_{2(1)}(\rho)$.

We assume the adiabatic limit for the fundamental mode, $\gamma_3 \gg \gamma_1,\gamma_2$, that allows us to operate effectively with two subharmonic modes. Indeed, in this limit of strongly dumped fundamental mode ω_3 the corresponding effective Hamiltonian reads as

$$H_{\mathrm{eff}} = i\hbar\frac{k\chi f(t)}{\gamma_3}(e^{i\Phi_k}b_1^\dagger b_2^\dagger - e^{-i\Phi_k}b_1 b_2), \quad (28)$$

while the master equation for the subharmonic modes (7) becomes

$$\frac{\partial\rho}{\partial t} = \frac{1}{i\hbar}[H_{\mathrm{eff}},\rho] + \sum_{i=1}^{3}\gamma_i(2b_i\rho b_i^* - b_i^\dagger b_i\rho - \rho b_i^\dagger b_i) + \frac{k^2}{\gamma_3}(2b_1 b_2\rho b_1^\dagger b_2^\dagger - b_1^\dagger b_1 b_2^\dagger b_2\rho - \rho b_1^\dagger b_1 b_2^\dagger b_2). \quad (29)$$

It is obvious that the appearance of the last term in this equation means that the influence of the adiabatically eliminated fundamental mode is also reduced to an additional loss mechanism for the subharmonic modes. In the undepleted pump approximation the last term in this equation should be omitted.

We perform calculations using the standard form of the Wigner functions in a Fock space

$$W_i(\rho,\theta) = \sum \rho_{i,mn}W_{mn}(\rho,\theta) \quad (i=1,2), \quad (30)$$

where ρ,θ are the polar coordinates in the complex phase-space plane and the coefficients $W_{mn}(\rho,\theta)$ are the Fourier transforms of matrix elements of the Wigner characteristic function.

Examples of both Wigner functions $W_1(\alpha)$ and corresponding distributions of quadrature amplitudes are plotted in Fig. 3 for the different time intervals within the pulsing period, which correspond to the minimum and maximum values of the photon numbers. As we see, the Wigner functions depend only on the radial coordinate $\rho=|\alpha|$, and are uniformly distributed with respect to the phase θ ($\alpha=\rho e^{i\theta}$). This radial symmetry is obvious and reflects the well-known phenomenon of phase diffusion occurring in NOPO.

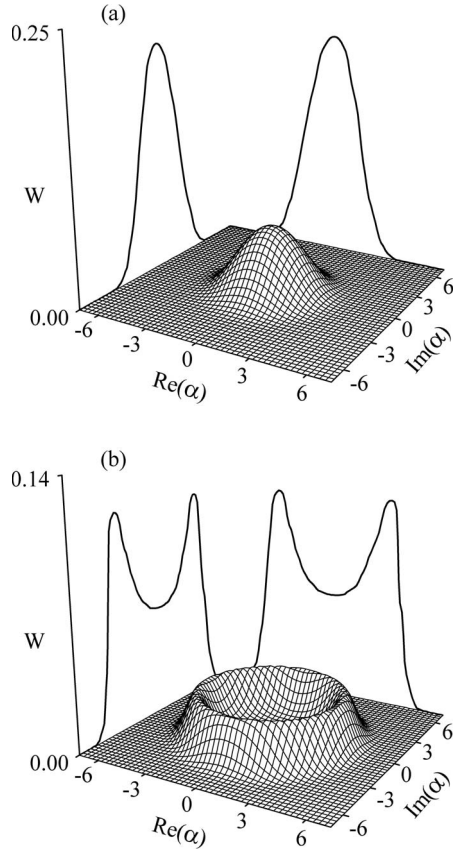

FIG. 3. Wigner functions for each of the modes at different times: (a) corresponds to time with minimal photon number and (b) for maximal photon number. The parameters are $\lambda=0.05\gamma$, $\chi=1.3\chi_{\mathrm{th}}$, $\tau=4\gamma^{-1}$, $T=1\gamma^{-1}$.

The one-mode Wigner function for NOPO under continuous-wave pump field was analytically calculated in [43]. Our results have similar form with this analytical result, however additionally contain some important details concerning nonstationary pulsed regime of NOPO. Clearly the Wigner function is non-Gaussian and hence the two-mode state from which it is derived is non-Gaussian as well.

We next calculate the Wigner function for the EPR beams by combining the correlated output modes (1) and (2) with a one-half beam splitter. This procedure is proposed here for verification of EPR entanglement in the time domain as a two-mode squeezing. Note that the opposite procedure is usually used for generation of CV entangled light beams. Indeed, it was demonstrated that quadrature entanglement can be achieved by linear interference of two intense amplitude squeezed modes on a beam splitter [44].

We consider the output behavior of NOPO assuming that all losses occur through the output couples [21]. In this case the output fields of subharmonics are $b_i^{\mathrm{out}}(t)=\sqrt{2\gamma}b_i(t)$ (i

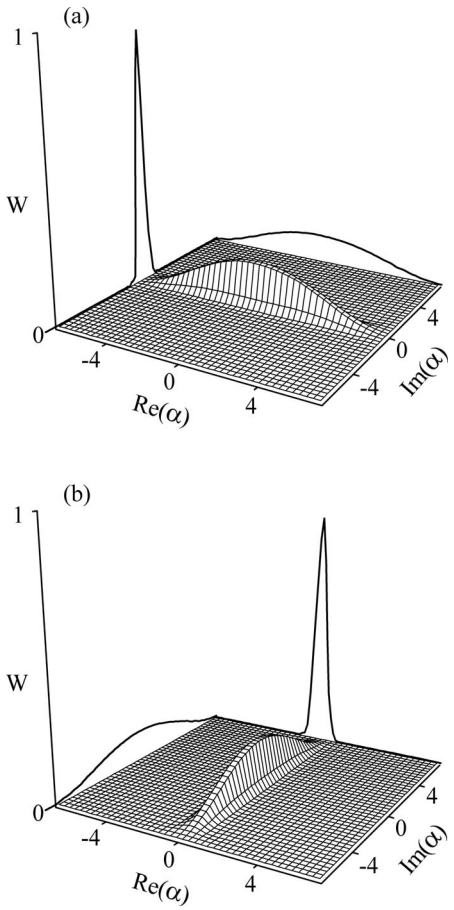

FIG. 4. Wigner functions for transformed coordinates: (a) mode $\alpha_1+\alpha_2$; (b) mode $\alpha_1-\alpha_2$. The parameters are $\lambda=0.05\gamma$, $\chi=1.3\chi_{\text{th}}$, $\tau=4\gamma^{-1}$, $T=1\gamma^{-1}$.

$=1,2$), and the output modes (b_A,b_B) from the one-half beam splitter can be expressed as

$$b_A=\sqrt{2\gamma}(b_1+b_2), \tag{31}$$

$$b_B=\sqrt{2\gamma}(b_1-b_2). \tag{32}$$

We present below the results for the Wigner functions $W_A(\alpha)$, $W_B(\alpha)$ of the combined, dimensionless modes $\alpha=\alpha_1+\alpha_2$, $\alpha=\alpha_1-\alpha_2$ corresponding to the operators $b_A/\sqrt{2\gamma}$, $b_B/\sqrt{2\gamma}$. The time evolution of the Wigner functions within the pulsing period $t_0+\tau$ is presented in Figs. 4 and 5.

A qualitative demonstration of strong EPR entanglement that is below the stationary limit is provided in Figs. 4(a) and 4(b), which show the Wigner function of the combined modes (A) and (B) for the time intervals corresponding to the maximal squeezing. Indeed, the qualitative measurement of the time-dependent squeezing effect can be revealed from our results by considering the quadrature amplitude probability distributions $P(x),P(y)[x=\text{Re}(\alpha),y=\text{Im}(\alpha)]$. Those are plotted in the backgrounds of Fig. 4. Note that probability distribution $P(x,\Phi)$ for any quadrature amplitude operator $X(\Phi)=\frac{1}{\sqrt{2}}(ae^{-i\Phi}+a^{\dagger}e^{i\Phi})$ can be obtained by integrating the Wigner function over the conjugate quadrature

$$P(x,\Phi)=\int_{-\infty}^{\infty}dpW(x\cos\Phi-p\sin\Phi,x\sin\Phi+p\cos\Phi). \tag{33}$$

In Fig. 4 we plot the marginal distributions $P(X)=P(x,0)$ and $P(Y)=P(x,\pi/2)$. The evolution of the Wigner function of (A) mode as well as the evolution of the quadrature amplitude distribution within the pulsing period is demonstrated in Fig. 5: (a) shows the Wigner function which is close to the Gaussian at $t=t_c-T$, where $t_c=t_0+i\tau(i\in\mathbb{Z})$ is a center point of the Gaussian pulse; (b) shows squeezed Wigner function evolved for a time $t=t_c$; and (c) and (d) show that after a time $t=t_c+0.75T$ two additional side humps are displayed. It should be noted that analogous two-humps structure displayed the Wigner function of a degenerate optical parametric oscillator (OPO) in the above-threshold regime (see, for example, [45]). These humps correspond to the states with equal numbers of photons and opposite phases. As we see from the formulas (13) with decreasing the parameter λ, the photon number involved in the above-threshold operational regime increases. In this regime the Wigner function (c) splits into two well-separated humps.

V. NEGATIVE WIGNER FUNCTIONS IN THE CONDITIONAL STATE-PREPARATION SCHEMES

In this section we consider Wigner functions of intensity-correlated twin beams following the conditional state-preparation scheme. According to the method of conditional measurement, counting n photons in one of the correlated modes projects the other mode in an n-photon Fock state, which can then be analyzed using quantum homodyne tomography. These measurements were recently demonstrated for one-photon Fock state $(n=1)$ [25,26] as well as for two-photon Fock state $(n=2)$ [27] by using a pulsed nondegenerate amplifier producing a pure two-mode squeezed state. The prepared states have been analyzed by a homodyne detection operating in a time-resolved regime. Here we consider this problem for the more general case that includes the full description of dissipative and pump field effects in the framework of the theory of periodically pulsed NOPO. The single-photon conditional measurement $(n=1)$, as well as both two-photon $(n=2)$ and three-photon $(n=3)$ measurement schemes, is considered. We assume that for the multiphoton cases, $n=2$ or $n=3$, the detection of coincidences by the photodiodes operating on a photon-counting regime mean that at least two-photon or three-photon states are created by the same pulse.

For this goal we calculate the conditional Wigner functions for light pulses if one of the modes (labeled trigger) is prepared in an n-photon Fock state $(n=1,2,3)$. When n-photon Fock state $|\psi_n(2)\rangle$ of the trigger mode (2) is detected, then the signal mode (1) is prepared in a quantum state whose density operator $\rho_1(n)$ reads as

$$\rho_1(n)=\frac{\langle\psi_n(2)|\rho|\psi_n(2)\rangle}{\text{Tr}\langle\psi_n(2)|\rho|\psi_n(2)\rangle}. \tag{34}$$

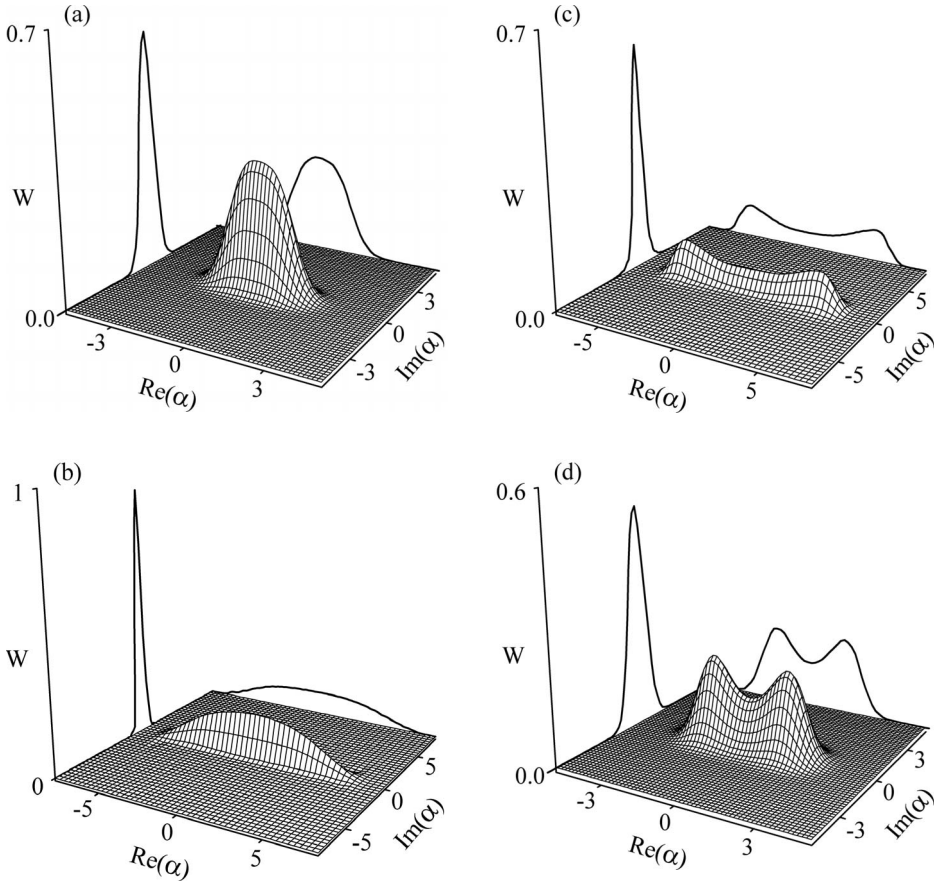

FIG. 5. Evolution of the Wigner function within the pulsing period for the parameters $\lambda=0.05\gamma$, $\chi=1.3\chi_{\text{th}}$, $\tau=4\gamma^{-1}$, $T=1\gamma^{-1}$: (a) $t=t_c-T$, (b) $t=t_c$, (c) $t=t_c+T$, (d) $t=t_c+2T$.

The resulting conditioned Wigner function of the output signal mode (1) is calculated on the formula analogous to Eq. (30),

$$W(n;\rho,\theta)=\sum_{m,p}\langle m(1)|\rho_1(n)|p(1)\rangle W_{mp}(\rho,\theta), \qquad (35)$$

where $|m(1)\rangle$ and $|p(1)\rangle$ are the Fock basis states of the mode (1).

We present the results of numerical calculations based on the QSD approach for the following Wigner functions: $W(1;\rho,\theta)$, $W(2;\rho,\theta)$, and $W(3;\rho,\theta)$ corresponding to the various conditional measurement schemes with $n=1$, $n=2$, and $n=3$ photon Fock states.

Examples of the Wigner functions for the below-threshold operational regime of NOPO are plotted in Fig. 6 for the time intervals within the pulsing period, which correspond to the maximum values of negativity. As we see, all three Wigner functions clearly display negative regions in the phase space that reflect a highly nonclassical character of quantum states. All Wigner functions are rotationally symmetric and hence the conditional mixed states are phase independent. In Fig. 7 we show the radial dependence of the Wigner functions. We stress that the results depicted in Figs. 6(a) and 6(b) are in agreement with the experimental and theoretical results on conditional Wigner functions $W(1)$ and $W(2)$ presented in [27]. Thus, the corresponding conditional mixed states are very close to one-photon and two-photon Fock states. The nonclassicality of the mixed states depicted in Figs. 6 and 7 are displayed as quantum interference effects. It is quite reasonable that these effects for the state preparation schemes based on pulsed NOPO are less than for the case of the photon pair generated in the process of parametric down conversion [26,27] or in an ideal nondegenerate amplifier producing a pure two-mode squeezed state [27]. The negative values of the Wigner functions $W(1)$, $W(2)$, and $W(3)$ decrease with increasing of the photon number of the signal mode. Nevertheless, as our analysis shows, the negativity of Wigner functions also takes place for the pulsed NOPO above threshold. However, in this regime the time intervals when the Wigner functions involve negative values correspond to a small number of photons. With increasing of the parameter χ (the intensity of the pump field) such time intervals become shorter. Thus, the time intervals where the Wigner functions contain negative values become shorter as well.

VI. CONCLUSION

In conclusion, we have studied the peculiarities of EPR light beams in the time domain. We have continued the recent investigation of periodically modulated NOPO and EPR entanglement [21] in one side and also we have considered the intensity-difference squeezing and the quantum distributions of EPR beams on the other side. We have proposed here a more realistic scheme generating nonstationary EPR beams, that is, a NOPO pumped by a sequence of Gaussian laser pulses. More importantly, we have seen that such

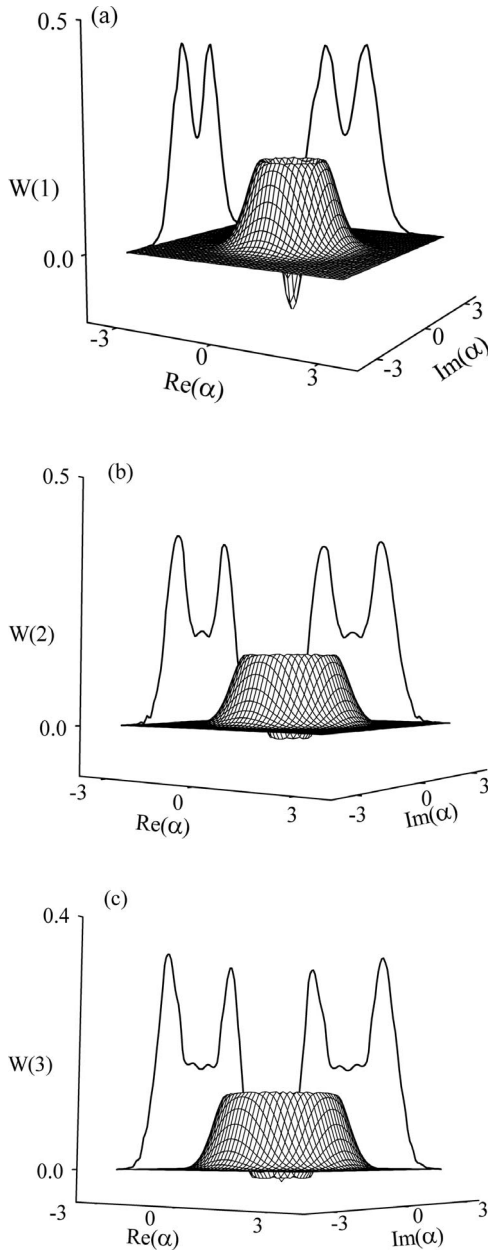

FIG. 6. Wigner functions and corresponding quadrature distributions for conditional measurement within the pulsing period for the parameters $\lambda=0.05\gamma$, $\chi=0.5\chi_{\text{th}}$, $\tau=4\gamma^{-1}$, $T=1\gamma^{-1}$: (a) $n=1$, (b) $n=2$, (c) $n=3$.

NOPO leads to formation of EPR beams with high degree of two-mode quadrature squeezing as well as intensity-difference squeezing. Indeed, we have demonstrated the operational regimes (depending on the durations of the pulses and the intervals between them) for which the level of the total squeezing, i.e., integrated on the spectral bandwidth squeezing, goes below the standard limit established for an ordinary NOPO with monochromatic pumping. We have demonstrated for the wide range of the parameters that the time-dependent quadrature variance $V(t)$ is equal to the normalized correlation function $G(t)$ describing photon-number-difference squeezing. Thus, we have concluded, that the CV entanglement in the time domain can be relatively easily demonstrated by direct measurement of the intensity-difference squeezing. More importantly, we have analyzed the evolution of various Wigner functions within the pulsing period. These results demonstrate a highly nonclassical character of mixed states generated in periodically pulsed NOPO.

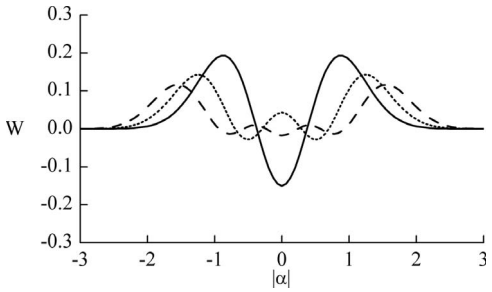

FIG. 7. Radial dependence of Wigner functions for conditional measurement for the parameters $\lambda=0.05\gamma$, $\chi=0.5\chi_{\text{th}}$, $\tau=4\gamma^{-1}$, $T=1\gamma^{-1}$: $n=1$ (solid line), $n=2$ (dashed line), $n=3$ (dotted line).

ACKNOWLEDGMENTS

The authors acknowledge helpful discussions with Olivier Pfister and M. Suhail Zubairy. This work was supported by NFSAT/CRDF Grant No. UCEP-02/07 and ANSEF Grant No. 666-PS-Opt.

APPENDIX: CALCULATION OF THE THRESHOLD

We calculate the threshold of generation for NOPO under a sequence of Gaussian pulses. For this goal we turn, at first, to integration of a periodic function.

Let us consider a periodic function constructed as follows:

$$g(t)=\sum_{n=-\infty}^{\infty} f(t+n\tau). \tag{A1}$$

It is easy to prove that

$$\int_0^{\tau} g(t)dt=\int_{-\infty}^{\infty} f(t)dt. \tag{A2}$$

Indeed,

$$F(t)=\int_{-\infty}^{t} f(\xi)d\xi, \tag{A3}$$

and we assume that $F(+\infty)=I<+\infty$.

Then

$$\int_0^{\tau} g(t)dt=\sum_{n=-\infty}^{\infty}\int_0^{\tau} f(t+n\tau)dt=\sum_{n=-\infty}^{\infty}[F((n+1)\tau)-F(n\tau)]$$
$$=F(+\infty)-F(-\infty)=I, \tag{A4}$$

because $F(-\infty)=0$.

Applying Eq. (A2) we obtain

$$\frac{1}{\tau}\int_0^{\tau}\chi_{\text{th}}f(t)dt=\frac{\gamma\gamma_3}{k}, \tag{A5}$$

$$\chi_{\mathrm{th}}\frac{T}{\tau}\int_{-\infty}^{\infty}e^{-t^2/T^2}dt/T=\frac{\gamma\gamma_3}{k}, \tag{A6}$$

$$\chi_{\mathrm{th}}=\frac{\gamma\gamma_3}{\sqrt{\pi}k}\frac{\tau}{T}=\frac{\gamma k}{\sqrt{\pi}\lambda}\frac{\tau}{T}. \tag{A7}$$

[1] M. D. Reid and P. D. Drummond, Phys. Rev. Lett. **60**, 2731 (1988); M. D. Reid, Phys. Rev. A **40**, 913 (1989).

[2] Z. Y. Ou, S. F. Pereira, H. J. Kimble, and K. C. Peng, Phys. Rev. Lett. **68**, 3663 (1992); S. F. Pereira, Z. Y. Ou, and H. J. Kimble, Phys. Rev. A **62**, 042311 (2000).

[3] Ch. Silberhorn, P. K. Lam, O. Weiß, F. König, N. Korolkova, and G. Leuchs, Phys. Rev. Lett. **86**, 4267 (2001).

[4] C. Schori, J. L. Sørensen, and E. S. Polzik, Phys. Rev. A **66**, 033802 (2002).

[5] W. P. Bowen, R. Schnabel, P. K. Lam, and T. C. Ralph, Phys. Rev. Lett. **90**, 043601 (2003).

[6] G. Yu. Kryuchkyan and L. A. Manukyan, Phys. Rev. A **69**, 013813 (2004).

[7] A. S. Villar, L. S. Cruz, K. N. Cassemiro, M. Martinelli, and P. Nussenzveig, Phys. Rev. Lett. **95**, 243603 (2005).

[8] X. L. Su *et al.*, Opt. Lett. **31**, 1133 (2006).

[9] J. Jing, S. Feng, R. Bloomer, and O. Pfister, Phys. Rev. A **74**, 041804(R) (2006).

[10] E. I. Mason and N. C. Wong, Opt. Lett. **23**, 1733 (1998).

[11] L. Longchambon, J. Laurat, T. Condrean, and C. Fabre, Eur. Phys. J. D **30**, 287 (2004).

[12] P. Groß, K. J. Boller, and M. E. Klein, Phys. Rev. A **71**, 043824 (2005).

[13] H. H. Adamyan and G. Yu. Kryuchkyan, Phys. Rev. A **69**, 053814 (2004); H. H. Adamyan, N. H. Adamyan, S. B. Manvelyan, and G. Yu. Kryuchkyan, *ibid.* **73**, 033810 (2006).

[14] G. Yu. Kryuchkyan and H. H. Adamyan, in *Strong Entanglement of Bright Light Beams in Controlled Quantum Systems*, edited by V. M. Akulin, A. Sarfati, G. Kurizki, and S. Pellegrin, NATO Science Series II: Mathematics, Physics and Chemistry, Vol. 189 (Springer, New York, 2005), p. 105.

[15] J. Laurat, T. Coudreau, and C. Fabre, Opt. Lett. **30**, 1177 (2005); J. Laurat, T. Coudreau, G. Keller, N. Treps, and C. Fabre, Phys. Rev. A **70**, 042315 (2004); **71**, 022313 (2005).

[16] S. Feng and O. Pfister, J. Opt. B: Quantum Semiclassical Opt. **5**, 262 (2003); Phys. Rev. Lett. **92**, 203601 (2004).

[17] J. Wenger, R. Tualle-Brouri, and P. Grangier, Opt. Lett. **29**, 1267 (2004).

[18] J. Wenger, J. Fiurášek, R. Tualle-Brouri, N. J. Cerf, and P. Grangier, Phys. Rev. A **70**, 053812 (2004).

[19] J. Wenger, A. Ourjoumtsev, R. Tualle-Brouri, and P. Grangier, Eur. Phys. J. D **32**, 391 (2005).

[20] A. Dantan, J. Cviklinski, M. Pinard, and Ph. Grangier, Phys. Rev. A **73**, 032338 (2006).

[21] H. H. Adamyan and G. Yu. Kryuchkyan, Phys. Rev. A **74**, 023810 (2006).

[22] N. Takei, N. Lee, D. Moriyama, J. S. Neergaard-Nielsen, and A. Furusawa, Phys. Rev. A **74**, 060101(R) (2006).

[23] D. T. Smithey, M. Beck, M. G. Raymer, and A. Faridani, Phys. Rev. Lett. **70**, 1244 (1993); D. T. Smithey, M. Beck, M. Belsley, and M. G. Raymer, *ibid.* **69**, 2650 (1992); A. Lvovsky and M. G. Raymer, e-print arXiv:quant-ph/0511044.

[24] A. E. B. Nielsen and K. Mølmer, Phys. Rev. A **76**, 033832 (2007); **75**, 043801 (2007).

[25] A. I. Lvovsky, H. Hansen, T. Aichele, O. Benson, J. Mlynek, and S. Schiller, Phys. Rev. Lett. **87**, 050402 (2001).

[26] A. Zavatta, S. Viciani, and M. Bellini, Phys. Rev. A **70**, 053821 (2004).

[27] A. Ourjoumtsev, R. Tualle-Brouri, and P. Grangier, Phys. Rev. Lett. **96**, 213601 (2006).

[28] M. Dakna, T. Anhut, T. Opatrny, L. Knoll, and D. G. Welsch, Phys. Rev. A **55**, 3184 (1997).

[29] J. S. Neergaard-Nielsen, B. M. Nielsen, C. Hettich, K. Mølmer, and E. S. Polzik, Phys. Rev. Lett. **97**, 083604 (2006).

[30] L. Mandel and E. Wolf, *Optical Coherence and Quantum Optics* (Cambridge University Press, Cambridge, 1995).

[31] F. Grosshans and P. Grangier, Eur. Phys. J. D **14**, 119 (2001); R. S. Bennink and R. W. Boyd, Phys. Rev. A **66**, 053815 (2002).

[32] T. Opatrný, N. Korolkova, and G. Leuchs, Phys. Rev. A **66**, 053813 (2002).

[33] M. Sasaki and S. Suzuki, Phys. Rev. A **73**, 043807 (2006).

[34] C. K. Law, I. A. Walmsley, and J. H. Eberly, Phys. Rev. Lett. **84**, 5304 (2000).

[35] K. J. Blow, R. Loudon, S. J. D. Phoenix, and T. J. Shepherd, Phys. Rev. A **42**, 4102 (1990).

[36] R. E. Slusher, Ph. Grangier, A. LaPorta, B. Yurke, and M. J. Potasek, Phys. Rev. Lett. **59**, 2566 (1987); P. Kumar, O. Aytur, and J. Huang, *ibid.* **64**, 1015 (1990); C. Kim and P. Kumar, *ibid.* **73**, 1605 (1994); M. E. Anderson, M. Beck, M. G. Raymer, and J. D. Bierlein, Opt. Lett. **20**, 620 (1995); E. M. Daly, A. S. Bell, E. Riis, and A. I. Ferguson, Phys. Rev. A **57**, 3127 (1998).

[37] D. F. Walls and G. J. Milburn, *Quantum Optics* (Springer-Verlag, Berlin, 1994).

[38] M. O. Scully and M. S. Zubairy, *Quantum Optics* (Cambridge University Press, Cambridge, 1997).

[39] A. Heidmann, R. J. Horowicz, S. Reynaud, E. Giacobino, C. Fabre, and G. Camy, Phys. Rev. Lett. **59**, 2555 (1987).

[40] J. Mertz *et al.*, Opt. Lett. **16**, 1234 (1991).

[41] J. Cao *et al.*, Opt. Lett. **23**, 870 (1998); H. B. Wang, Y. Zhang, Q. Pan, H. Su, A. Porzio, C. Xie, and K. Peng, Phys. Rev. Lett. **82**, 1414 (1999); H. B. Wang, Europhys. Lett. **64**, 15 (2003).

[42] G. Yu. Kryuchkyan, K. G. Petrosyan, and K. V. Kheruntsyan, Pis'ma Zh. Eksp. Teor. Fiz. **63**, 502 (1996).

[43] K. V. Kheruntsyan and K. G. Petrosyan, Phys. Rev. A **62**, 015801 (2000).

[44] A. Furusawa *et al.*, Science **282**, 706 (1998); T. C. Ralph and P. K. Lam, Phys. Rev. Lett. **81**, 5668 (1998); G. Leuchs, T. Ralph, C. Silberhorn, and N. Korolkova, J. Mod. Opt. **46**, 1927 (1999).

[45] K. V. Kheruntsyan, D. S. Krähmer, G. Yu. Kryuchkyan, and K. G. Petrossian, Opt. Commun. **139**, 157 (1997).